

Vibrational Spectra, Phase Transitions and Conformers of 1,4-Dichlorobut-2-yne

A. Karlsson, P. Klæboe* and C. J. Nielsen

Department of Chemistry, University of Oslo, 0315 Oslo 3, Norway

The Raman and IR spectra of 1,4-dichlorobut-2-yne (DCB) as a liquid at various temperatures and as an amorphous and as metastable and stable crystalline solids at low temperatures have been recorded in the 4000–20 cm⁻¹ range. Additional IR and Raman spectra of a high-pressure crystalline phase were obtained at ca 17 kbar pressure.

The broad unsymmetrical bands of DCB in the liquid and in the amorphous solid below 500 cm⁻¹ suggest nearly free rotation in these phases at all of the temperatures investigated. Below ca 190 K a crystal containing the *anti* and above 190 K a crystal containing the *gauche* conformer of DCB were formed; the latter crystal is believed to be thermodynamically more stable at all temperatures. Only one high-pressure crystal with molecules in the *anti* conformation was formed at room temperature. A phase transition reported at 232 K in the liquid, involving a conversion to an *anti* conformer, was not detected.

Complete vibrational assignments for both *anti* and *gauche* conformers are presented, supported by force constant calculations.

INTRODUCTION

Molecules of 1,4-dihalobut-2-yne have attracted considerable attention because of their low barrier to internal rotation. Consequently, the conformations of these molecules are not as straightforward as those in the ethanes. In addition to the staggered conformers *anti* and *gauche* with large torsional amplitudes and possibly also the eclipsed *syn*, the molecules may exhibit essentially free internal rotation. Despite a low potential barrier, the 1,4-dihalobut-2-yne are expected to be locked in distinct conformers in the crystalline state. In the vapour and liquid states we expect essentially free rotation, and possibly distinct conformers in the low-temperature amorphous phase, depending on the temperature and the barrier height relative to $k_B T$. These molecules should be studied over a wide temperature range in all of the states of aggregation, investigations which can be carried out by vibrational spectroscopy.

In this laboratory we have been interested in the 1,4-dihalobut-2-yne for some time, and the dibromo compound was studied by electron diffraction¹ and by vibrational spectroscopy² several years ago. Recently, our results for 1,4-difluorobut-2-yne obtained by IR, Raman and microwave spectroscopy were published,³ revealing a higher barrier for this molecule. In this paper we report a Raman and IR spectroscopic study of 1,4-dichlorobut-2-yne (DCB).

DCB has been studied by various methods, including dipole moments in solution⁴ and in the vapour phase.⁵ The structure was determined by electron diffraction^{6,7} from the vapour, indicating a negligible barrier to internal rotation. Following earlier Raman⁸ and IR⁹ investigations, Bak *et al.*¹⁰ obtained new data for the liquid and interpreted the spectra in terms of D_{3d} pseudo symmetry (free rotation). Crowder¹¹ carried out a force constant calculation that suggested accidental degeneracy in several vibrations of the CH₂Cl groups.

* Author to whom correspondence should be addressed.

The large band widths below 500 cm⁻¹ of the vapour and liquid spectra were interpreted as being due to nearly free rotation¹¹⁻¹³ in DCB.

Two conformers of DCB, *anti* and the *gauche*, were subsequently formed by Mannik *et al.*¹⁴ in the crystal. The conformer obtained reportedly¹⁴ depended on the thermal history of the sample and on the properties of the container surface. The same group¹⁵ claimed a novel type of liquid-liquid phase transition in DCB in which a conformational mixture is suddenly converted into a single conformer liquid. The phase transition reportedly took place around 233 K either as a liquid in a glass capillary or as a film between rubbed flat glass surfaces leading to an *anti* conformer. Finally, Suzuki¹⁶ obtained the two crystals containing the *anti* or the *gauche* conformers by cooling to different temperatures and also recorded a matrix isolation spectrum.

In spite of these efforts, we felt that a thorough understanding of the phase transitions in crystalline DCB was missing. In particular, the liquid-liquid phase transition reported¹⁵ seemed to be highly sensational and well worth a repeated investigation. Therefore, we have made a thorough study of the Raman and IR spectra of DCB in various phases at different temperatures, including high-pressure crystallization at ambient temperature. The IR spectra were extended to 30 cm⁻¹, where we observed a number of IR active modes previously not detected. A complete assignment of the fundamentals to the liquid (free rotation) and to the *anti* and *gauche* conformers is presented, supported by a force constant calculation.

EXPERIMENTAL

The sample of DCB, containing a small amount of water, was obtained from Aldrich. After distilling the sample over P₂O₅ on a vacuum line, the product was greater than 99.5% pure according to a gas chromatographic analysis.

The IR spectra were recorded with a Perkin-Elmer Model 225 ($4000\text{--}200\text{ cm}^{-1}$) and a Bruker FTIR Model 114 c ($4000\text{--}20\text{ cm}^{-1}$) evacuable spectrometer. Sealed cells with windows of KBr and polyethylene were employed for the neat liquid and solutions. The use of CsI windows was avoided at ambient temperature since a pink colour developed, suggesting reactions. Moreover, DCB should not come into contact with steel, since impurity peaks appeared in the spectra when metal syringes were employed. Cryostats with CsI and silicon windows were used at liquid nitrogen temperature. A commercial cryostat from RIIC with an inner sandwich cell with AgCl windows was used in the temperature range 298–200 K. High-pressure IR spectra (and incomplete Raman spectra) were obtained with a diamond anvil cell (DAC) with type IIa anvils, combined with a Perkin-Elmer 4x beam condenser.

Raman spectra were recorded with a Dilor Model RT 30 triple monochromator spectrometer interfaced with the Aspect 2000 computer of the Bruker spectrometer. Argon ion lasers from CRL (Model 52 G) and from Spectra-Physics (Model 2000) with 90° and 180° scattering geometries, using the 514.5 and 488.0 nm lines, were employed for excitation. Polarization measurements of the neat liquid in 1 cm fluorescence cells were made.

Various cooling techniques following reported procedures^{14–16} were employed in the Raman experiments. Capillaries of 3 and 1 mm i.d., surrounded by a Dewar vessel and cooled by cold nitrogen gas¹⁷ were employed in the 270–180 K range. A Raman sandwich cell made of glass plates (5×20 mm) rubbed with tissue paper and separated by a 0.5 mm PTFE spacer like the cell described by Sipos and Phibbs¹⁵ was cooled in the same Dewar vessel¹⁷ and illuminated in the 90° and 180° modes. In another Raman cryostat the vapour of DCB was sprayed on a copper finger, cooled with liquid nitrogen, subsequently annealed at higher temperatures and recooled to 90 K before recording.

DCB as a neat liquid was studied visually between crossed polarizers in the following vessels: (1) a melting-point tube of 0.6 mm i.d., (2) a tube of silica of 5 mm i.d. and (3) as a capillary film between glass plates with a layer of oblique evaporated silicon oxide used for liquid crystal displays.¹⁸ The sample was studied in the temperature range 290–115 K.

A Perkin-Elmer Model DSC 1 B differential scanning calorimeter cooled with liquid nitrogen was used to obtain heating and cooling curves for DCB. Further investigations of the solid phases were carried out with a low-temperature x-ray Guinier Simon camera from Enraf Nonius (Model FR 553), which was employed in a cooling (270–140 K) and a heating cycle (140–270 K).

RESULTS

Low-temperature solids and spectra

At a cooling rate of 4°C min^{-1} the difference scanning calorimeter (DSC) curve gave a peak at 198 K, whereas the heating curve gave a peak at 243 K (Fig. 1). Heating curves recorded at different heating rates in the range $2\text{--}8^\circ\text{C min}^{-1}$ gave essentially the same value for the melting point (243 K). The freezing point varied slightly

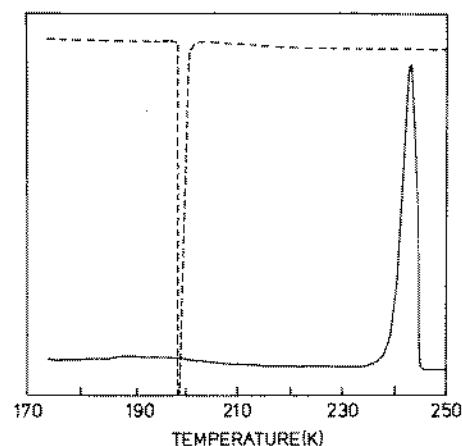


Figure 1. Differential scanning calorimeter (DSC) traces of cooling (dotted line) and heating curves (solid line) of DCB.

with each curve. No additional peaks attributed to phase transitions were detected in the 270–160 K range accessible with the DSC instrument.

In the x-ray experiments the cooling and heating rates were $0.25^\circ\text{C min}^{-1}$. As is apparent from Fig. 2, sharp x-ray patterns due to crystallization occurred at 173 K during the cooling process. The heating curve showed a phase transition at 201 K before melting at 243 K.

Various procedures for crystallizing DCB were attempted in order to gain an insight into the different phases formed. Infrared and Raman spectra are shown in Figs 3–6.

Shock freezing the vapour. (a) The vapour of DCB was shock frozen on CsI (mid-IR) and silicon windows (far-IR) or on a copper plate (Raman) at 90 K. Amorphous IR and Raman spectra were invariably obtained (Figs 3 and 4(a)), similar to those for the liquid (Figs 9 and 10). (b) When the temperature was increased, first no spectral changes occurred and the spectra remained amorphous. Above 150 K the solid deposit turned frosty, and spectral variations were observed. After 15–30 min in the range 150–185 K, a complete conversion to crystal

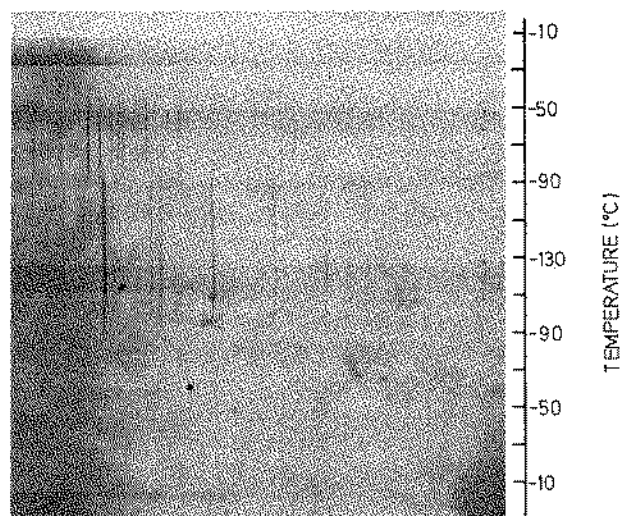


Figure 2. X-ray Guinier Simon diffractogram of DCB in a cooling (263–143 K) (bottom) and a heating cycle (143–263 K) (top).

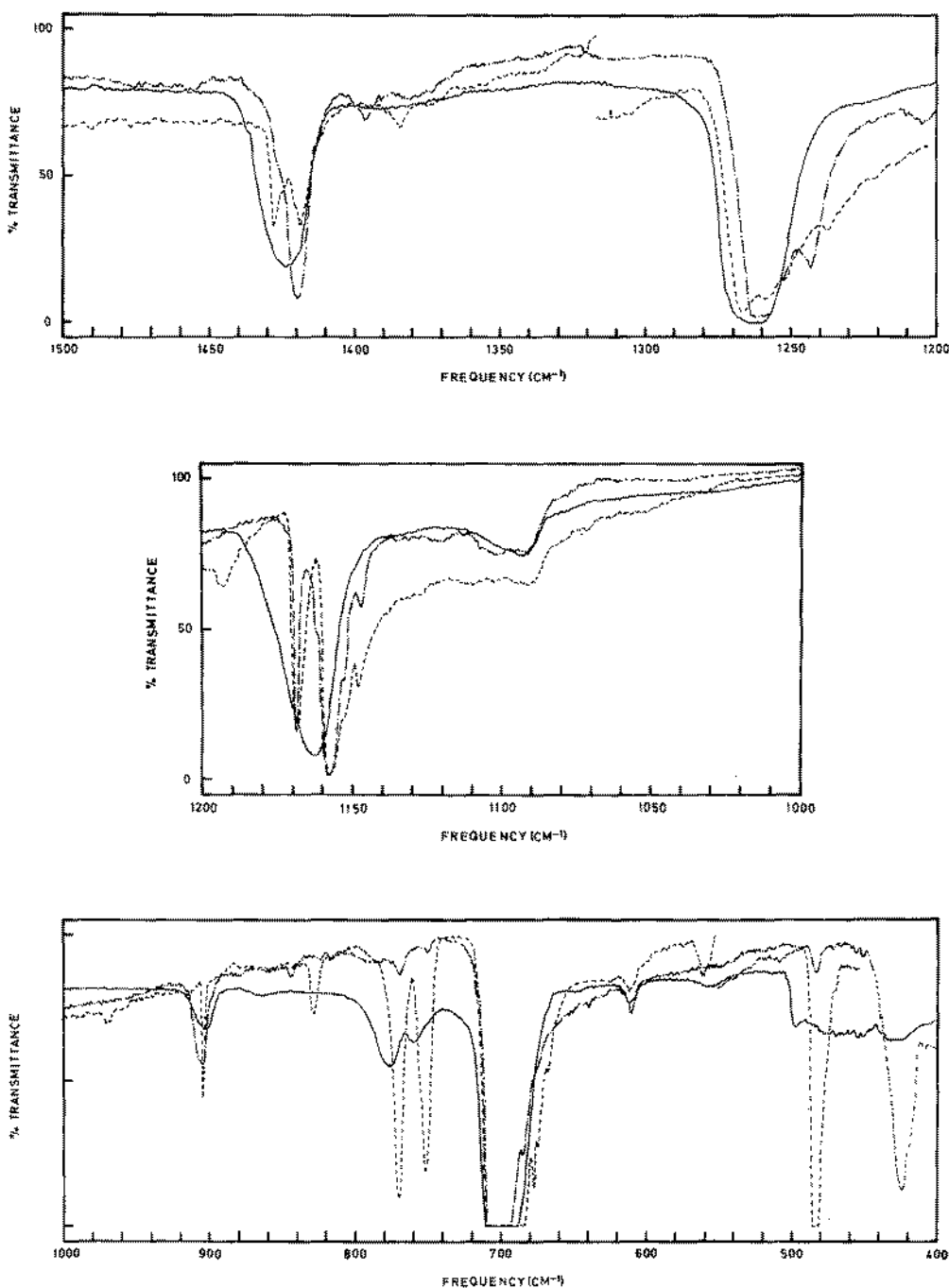


Figure 3. Infrared spectra of DCB at 90 K. —, Amorphous solid; - - - -, crystal I with Molecules in *anti* conformation; and - · - · -, crystal II with molecules in *gauche* conformation.

I took place. No spectral changes happened when the sample was recooled to 90 K (Fig. 3, - · - · -). (c) When the amorphous phase was heated above 190 K a mixture of crystals I and II was formed, but above *ca* 200 K crystal II was formed directly. (d) When the pure crystal I formed as described under (b) was heated above *ca* 200 K a slow conversion to crystal II occurred, as previously reported.¹⁴ (e) When crystal II was formed no conversion to crystal I was achieved by cooling.

Cooling the liquid. (a) Capillary tubes of 2 and 1 mm i.d. were immersed in a Dewar vessel and cooled with cold nitrogen gas.¹⁷ When cooled slowly, DCB usually crys-

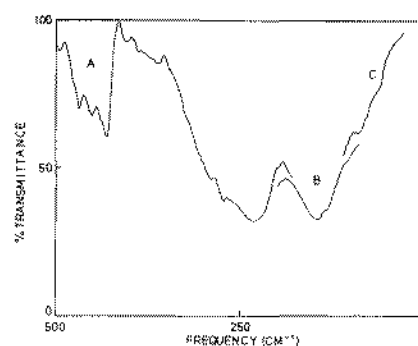
tallized around 238 K, invariably forming crystal II. Thus, the supercooling was considerably less in the glass capillaries than in the metal holders for DSC (Fig. 1) or in the quartz tube employed for the x-ray recordings (Fig. 2). When the capillaries were cooled rapidly, considerable supercooling occurred and the DCB crystallized at *ca* 185 K into crystal I. (b) DCB was confined between 1 mm thick glass plates rubbed unidirectionally with tissue paper using a 0.5 mm thick PTFE spacer.¹⁵ With slow or rapid cooling procedures, crystals II and I were formed, respectively. The crystallization was similar when DCB was confined between rubbed glass plates or in glass tubes of different diameters. The

molecules in crystal I were partly oriented, as is apparent from the relative band intensities in Fig. 7, obtained with the plane of polarization parallel and perpendicular to the rubbing direction. (c) When DCB was confined in a sandwich cell with AgCl windows, crystal II was invariably formed on cooling, as is apparent from the IR spectra. The heat transfer was slower than in the Raman experiments (a) and (b), therefore leading to crystallization at a higher temperature.

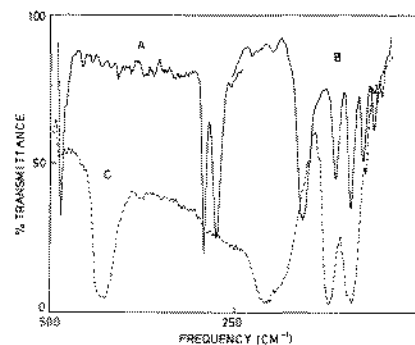
High-pressure spectra

When compressed in the DAC, liquid DCB had IR spectra identical with those obtained at atmospheric pressure, neglecting a small displacement towards higher wavenumbers of the band maxima. No changes in the broad IR bands below 500 cm^{-1} were observed, suggesting that the low barrier is maintained under high pressure. In a polarizing microscope the liquid appeared isotropic with no unexpected features.

At *ca* 17 kbar the liquid spontaneously crystallized to a polycrystalline solid, as seen in a polarization microscope. The IR spectrum of the high-pressure crystal was similar to that of crystal I recorded at low temperature (Fig. 8). The pressure was increased above 50 kbar without any phase changes taking place, and no crystal II was ever obtained by high-pressure crystallization at ambient temperature. When the pressure was reduced the sample melted, and crystal I was repeatedly formed on increasing the pressure again.



(a)



(b)

Figure 4. Far-infrared spectra of DCB at 90 K. (a) Amorphous solid recorded with different beam splitters; (b) crystal I (curve C) and crystal II (curves A and B).

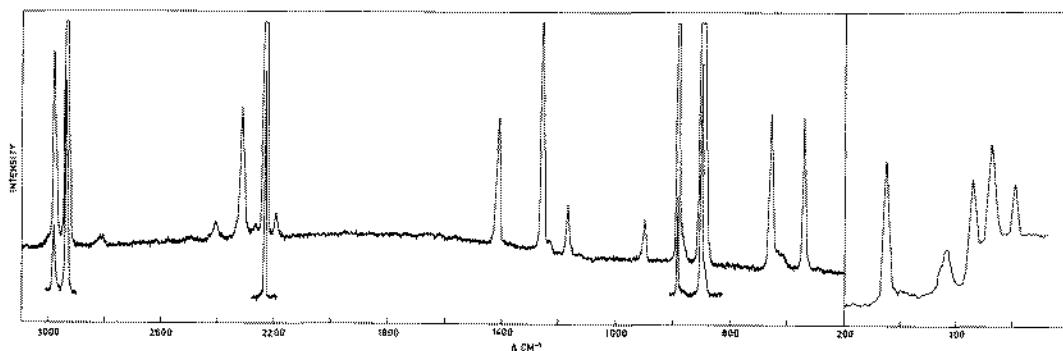


Figure 5. Raman spectrum of DCB at 90 K. Crystal I with molecules in *anti* conformation.

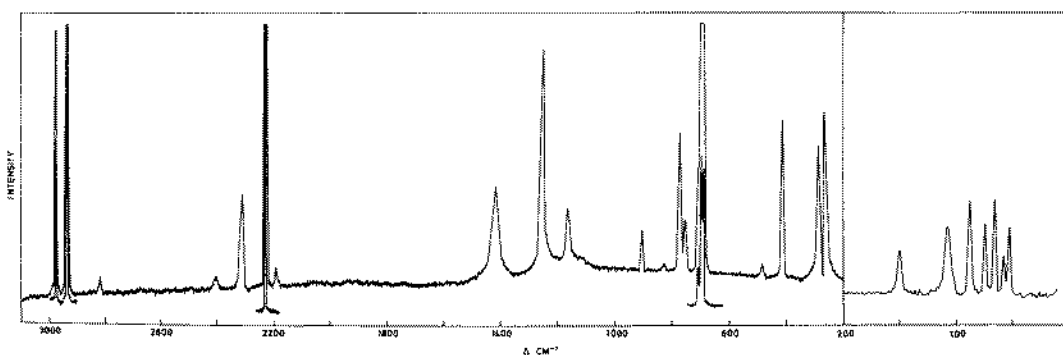


Figure 6. Raman spectrum of DCB at 90 K. Crystal II with molecules in *gauche* conformation.

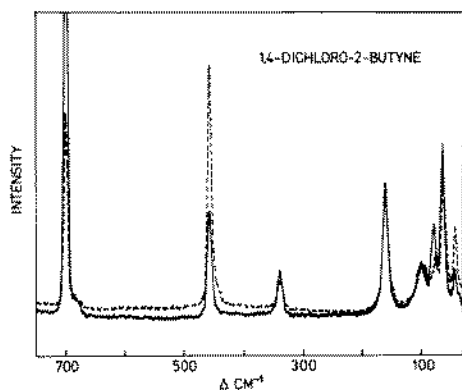


Figure 7. Raman spectra of DCB between rubbed glass plates. Sample thickness, 0.5 mm; 190 K; electric vector of laser beam parallel (dotted line) and perpendicular (solid line) to rubbing direction; 180° illumination mode.

Liquid-phase spectra

The IR and Raman spectra of DCB as a neat liquid at ambient temperature are given in Figs 9 and 10, respectively. Earlier workers^{10,11,15} noticed that the broad bands observed below 500 cm^{-1} were quite different from those of the crystal spectra.

Sipos and Phibbs¹⁵ reported that DCB as a liquid is converted from a mixed conformational state (rather a conformer with nearly free rotation) to a pure *anti* conformer over a small temperature interval. The effect was

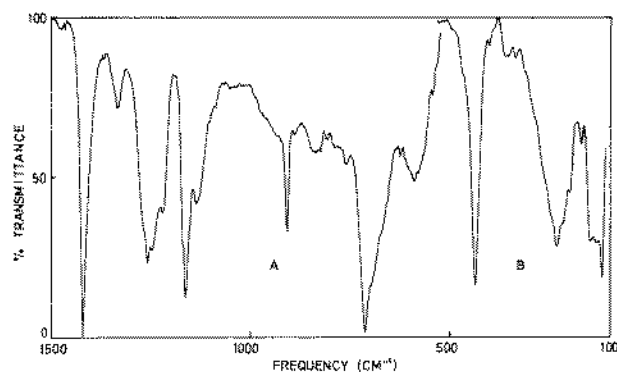


Figure 8. Infrared spectrum of DCB at ambient temperature under ca 17 kbar pressure in a diamond anvil cell (DAC) giving crystal I.

reportedly dependent on the orientational order of the surface vessel. For these reasons a large number of experiments were carried out in which the liquid, confined in different cells and capillary tubes, was cooled to temperatures just above the crystallization temperature. Hence the cooling procedures used to crystallize the liquid described above in the section cooling the liquid (a-c) were followed, but the liquid or super-cooled liquid rather than the crystals was studied. It should be emphasized that in our Raman spectrometer with horizontal slits and laser beam it can be definitely decided if the sample is liquid or crystalline. After passing through the glass Dewar vessel and the sample

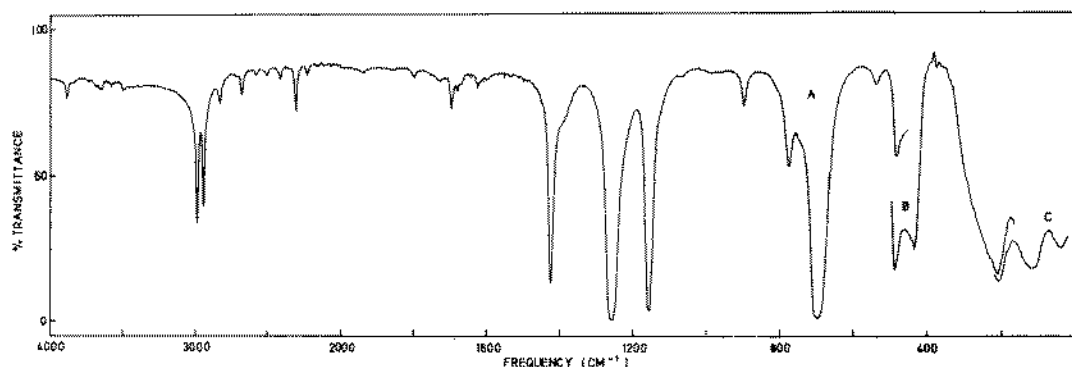


Figure 9. Infrared spectrum of DCB. (A) Capillary film of neat liquid; (B and C) 10% solution in C_6H_{12} , 1 mm path with PET windows with 3.5 and $12\ \mu\text{m}$ beam splitters.

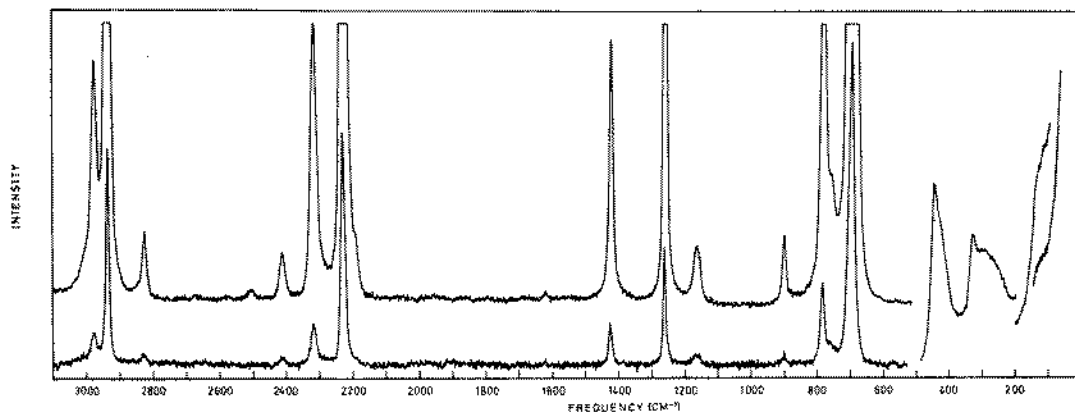


Figure 10. Raman spectrum of liquid DCB at 295 K.

(confined in a capillary or as a film between glass plates), the laser beam makes a pattern on the laboratory walls completely different for liquid and crystalline samples. Moreover, in our vertical Miller-Harney type cell,¹⁷ used horizontally by the earlier workers,¹⁵ a considerable temperature gradient was present. At temperatures around the melting point the bottom part of the sample standing in the laser beam was crystalline, whereas the top part was a liquid.

In our preliminary experiments a cloudiness of DCB at temperatures around 233 K was detected, as described by Sipos and Phibbs.¹⁵ However, this effect was not due to optical anisotropy (like the appearance in nematogens) but was caused by ice crystals. When DCB was distilled over P₂O₅ the cloudiness disappeared completely.

In 30–40 independent measurements with cooled liquids using IR and Raman spectroscopy no effects like those reported by Sipos and Phibbs¹⁵ were detected. The liquid invariably gave spectra like those obtained at room temperature (Figs 9 and 10) with slightly sharper contours. In no case had the IR or Raman spectra of cooled, liquid DCB an appearance like the reported *anti* spectrum.¹⁵

The visual studies of DCB in glass capillaries or in the sandwich cell suitable for orienting nematic and smectic liquid crystals¹⁸ gave no unexpected effects between crossed polarizers. Thus, DCB appeared isotropic in the liquid state until the freezing point.

DISCUSSION

Crystalline state

As reported by earlier workers,^{14–16} two crystals of DCB can be formed on cooling (crystals I and II). The x-ray scattering data (Fig. 2) reveal different crystal structures in the two phases, as is also apparent from the lattice modes (Figs 5 and 6). Crystal I contains molecules in the *anti* conformer (molecular point group C_{2h}) and crystal II consists of molecules in the *gauche* conformer (C_2 symmetry). There are no reversible phase transitions between the two crystals; crystal II appears to be thermodynamically more stable at all temperatures (at atmospheric pressure). Crystal I is metastable but can be maintained for hours (and maybe for days) at temperatures below 178 K. Above this temperature crystal I slowly converts to crystal II. As seen from the x-ray results (Fig. 2) and Fig. 2 in Ref. 14, the conversion is rapid at *ca* 193 and 208 K, respectively.

It is not possible to give any meaningful transformation temperature for an irreversible phase transition. Kinetic factors are highly important and the transitions will be functions of both time and temperature. One can merely define a temperature below which an irreversible transformation does not take place,¹⁸ apparently being close to 185 K for DCB.

In our experiments, crystal II was invariably formed when DCB as a liquid was slowly cooled and the crystallization occurred with relatively minor supercooling. We also obtained crystal II when the amorphous substance, shock frozen at *ca* 90 K, was annealed above 200 K.

Crystal II was definitely thermodynamically stable and was never converted to crystal I at atmospheric pressure.

Crystal I was formed when liquid DCB was cooled rapidly with greater supercooling and the crystallization occurred below *ca* 190 K. Correspondingly, the shock-frozen amorphous solid formed at 90 K gave crystal I with careful annealing below 185 K. Unlike Mannik *et al.*,¹⁴ we found no significant difference depending on the size, orientational surface order of the vessel or of the thermal history of the liquid before crystallization. Thus, capillaries of different diameters, liquid films between rubbed glasses or IR cells all gave the same results.

The possible effect on the crystallization derived from the vessel depends, in our opinion, on the extent of supercooling before crystallization. DSC, x-ray experiments and crystallization in glass capillaries clearly demonstrate varying degrees of supercooling. Cells giving considerable supercooling should make it easier to give crystal I. In the x-ray experiments (Fig. 2) the great supercooling in the quartz tube led to the formation of crystal I at 173 K on cooling. The heating cycle gave a crystal I–crystal II phase transition at 201 K. The DSC cooling curve apparently gave crystal II at 198 K, since no phase transitions were observed in the heating curve (Fig. 1).

We believe the liquid DCB to be isotropic until crystallization, and the length of time it is kept at a certain temperature (e.g. 233 K¹⁴) should therefore be irrelevant. These results are in good agreement with those of Suzuki,¹⁶ taking into account that her fast deposition at 15 K probably heated the cryostat considerably so that crystal I was obtained directly.

The high-pressure crystal obtained at *ca* 17 kbar invariably gave crystal I consisting of the *anti* conformer. Generally, conformers with smaller molar volumes are favoured under high pressure, as observed e.g. for 1,1,2-trichloroethane.^{20,21} However, for DCB the *anti* conformer should probably have a larger volume than the *gauche* conformer, although more efficient packing in the *anti* crystal can explain the behaviour observed.

Our results concerning the crystallization and conformations of DCB in the crystals are parallel to those reported earlier for *trans*-1,4-dihalocyclohexanes.^{22,23} Thus, all six derivatives ClCl, ClBr, ClI, BrBr, BrI and II have a stable crystal with the molecules in the *ee* conformation. A metastable crystal with molecules in the *aa* conformation can be obtained by annealing the amorphous solid at lower temperatures.^{21,22} At higher temperatures the *aa* conformer crystal converts into the '*ee* crystal,' which remains stable at all temperatures.

In the high-pressure crystal of 1,4-dihalocyclohexanes the conformation is *aa*,^{22,23,24} again parallel to the behaviour of DCB. Still another example is provided by 1-cyanobut-3-yne,²⁵ which gives a metastable crystal, probably *gauche*, when annealed to 140 K and a stable crystal of *anti* conformation when annealed to 190 K.

Liquid state

Unlike 1,4-difluorobut-2-yne,³ DCB and 1,4-dibromobut-2-yne^{1,2} have very broad IR and Raman bands below 500 cm⁻¹ in the liquid-state spectra, interpreted^{10–12} as a result of nearly free internal rotation.

The band shapes are nearly the same in spectra of the supercooled liquid around 230 K and in the amorphous deposit at 90 K.

The spectroscopic selection rules for DCB with nearly free rotation are not known (see below), but in the liquid and vapour phases⁴⁻⁷ DCB is therefore present neither as *anti* nor *gauche* but as molecules characterized by the MS group D_{2h}^* .²⁶

The present results have in no way reproduced the spectroscopic results of Sipos and Phibbs¹⁵ concerning the existence of a liquid-state phase transition for DCB. Following their procedures meticulously and making numerous other attempts, we were never able to observe an *anti* spectrum of DCB in the liquid state at any temperature or in any type of cell.

The conformational equilibrium in the vapour phase and in the liquid is determined by the enthalpy and entropy differences between the conformers, ΔH and ΔS , giving the Gibbs free energy $\Delta G = \Delta H - T\Delta S$. Thus, a sudden conversion to one conformer in the liquid is not thermodynamically feasible unless intermolecular energy terms contribute, as they do in the crystalline state. Accordingly, Sipos and Phibbs¹⁵ implicitly explain their findings by assuming nematogenic (non-isotropic) behaviour of DCB around 233 K. Our visual observations of DCB confined in capillary tubes of various diameters and between rubbed glass plates, especially suitable for orienting nematogens,¹⁸ showed completely isotropic behaviour between crossed polarizers. The capillaries and the sandwich cells with rubbed glass windows also showed no apparent birefringence in the laser beam.

We do not believe that DCB is a nematogenic compound, for the following reasons.

Nearly all the known thermotropic liquid crystals have (1) a cyclic core consisting e.g. of benzene and/or cyclohexane, (2) a polar group such as cyanide or methoxy and (3) a flexible hydrocarbon chain.²⁷ DCB lacks all these prerequisites and all the known compounds forming nematic, smectic or cholesteric mesophases are unsymmetrical and have by far a more complicated structure than DCB. Below their clearing point nematogens have a turbid appearance owing to their birefringence. However, the cloudiness reported¹⁵ on cooling DCB, also detected by us, disappeared completely after drying and was probably caused by ice crystallites.

From NMR²⁸ and IR²⁹ measurements an increased probability of all-*trans* conformers of the hydrocarbon chain are reported in the nematic compared with the isotropic phase in certain nematogens. However, to our knowledge there are no examples in the literature in which a nematogen is converted into a single conformer below the clearing point. Hence, in the very unlikely case that DCB should be a nematogen, the reported¹⁵ conformational behaviour would still be highly unexpected.

For these reasons we believe that the liquid-phase transition for DCB at 232 K, reportedly dependent on the surface of the cell,¹⁵ is an artifact. Instead, it seems likely that the reported¹⁵ Raman spectra of the *anti* conformer are not obtained in the liquid but in the crystalline state. The temperature gradient observed in our vertical Dewar vessel¹⁷ is probably also present in their horizontal¹⁵ set-up and makes this assumption very

probable. Also, the reported dichroism of the liquid sample between rubbed glass plates (Fig. 2 in Ref.¹⁵) agrees fairly well with our crystal I spectra (Fig. 7). However, the intensity ratio between the bands at 698 and 455 cm^{-1} is opposite relative to the rubbing direction in the earlier¹⁵ and in our spectra. Apparently, the molecular orientation is different relative to the rubbing direction in the two studies. Lastly, the narrow peaks observed in their Raman spectra at 232 K definitely suggest a crystal spectrum in which the molecules are locked in the *anti* conformer by the crystal lattice. The supercooled and amorphous spectra recorded at much lower temperatures all have the broad band features. We cannot explain their *anti* conformer in these spectra unless their sample was previously cooled below 200 K. All our experiments led to crystal II (*gauche*) by the careful freezing around 232 K and crystal I (*anti*) formed with large supercooling.

Spectral interpretation

Very good Raman spectra of the two crystals, including the low-frequency region, were recorded by Suzuki,¹⁶ but the far-IR region has not been recorded previously. Thus, with the large amount of data now available for DCB a complete spectral interpretation should be feasible. The assignments are listed with the experimental data in Table 1, whereas the *anti* and *gauche* conformers of the two crystals are listed in Tables 2 and 3, respectively.

In 1,4-difluorobut-2-yne³ the barriers were found by microwave spectroscopy to be 4.1 and 2.2 kJ mol^{-1} for the *syn* and *anti* conformers, respectively. The vibrational bands for this molecule did not change significantly on crystallization. Broad bands were present in the spectra of amorphous DCB at 90 K, and the barrier must be below $\exp(-\Delta E/kT)$ kJ mol^{-1} for this molecule.

In the Longuet-Higgins formalism, DCB should in the liquid (and vapour) belong to the molecular symmetry (MS) group D_{2h}^* .²⁶ Attempts were made to derive the general selection rules for IR and Raman activity and the Raman polarization ratios for this MS group. However, since the actual symmetry of the normal coordinates remained unknown, no definite results were obtained. The structure of DCB in the MS group D_{2h}^* is $\Gamma_{\text{vib}} = 8a_{1g} + 4a_{2g} + 4b_{1g} + 7b_{2g}$. Mixing of symmetry coordinates from different species³⁰ makes it feasible to distinguish normal coordinates of the *a*-type species from the *b*-type species. The spectra indicate that both (all) are active in IR and in Raman.

The solid-state spectra of crystals I and II reveal beyond doubt that DCB has a definite conformation in these lattices. As reported earlier,¹⁴⁻¹⁶ the IR and Raman selection rules are in agreement with C_{2h} (*anti*) and C_2 (*gauche*) symmetry in these crystals. In crystal I the normal modes divide themselves between $8a_g + 4b_g + 5a_u + 7b_u$ and mutual exclusion is clearly seen in the spectra. The IR and Raman bands generally coincide in crystal II and the molecular symmetry would be C_2 for a general dihedral angle and C_{2v} for 0° angle (*syn*). With C_{2v} symmetry the four a_2 modes should be Raman active and IR inactive. No such non-coincidences were observed with certainty and the calculated frequencies do fit a dihedral angle between 60 and 100° (99° from

Table 1. IR and Raman spectral data for 1,4-dichlorobut-2-yne

Liquid		Amorphous (90 K)		Crystal I (90 K)		Crystal II (90 K)		Crystal I high pressure		Assignments ^a			
IR	Raman	IR	Raman	IR	Raman	IR	Raman	IR	Raman	C_{2h}	C_2	D_{2h}^*	
2994 s ^b	2994 s, D	2998 s	2996 m	2998 s	3002 s	2992 w	2995 s/m	3019 s	3020 s	$\nu_1(a_g)$	$\nu_9(b_g)$	$\nu_1(a), \nu_{13}(b)$	
2953 s	2953 vs, P		2952 m	2958 m	2956 s	2952 w	2953 s	2952 w	2970 vs	$\nu_{18}(b_u)$	$\nu_1(a_g)$	$\nu_2(a), \nu_{16}(b)$	
2842 w	3844 m	2920 w ~2850 w, bd	2835 vw	2822 vw	2822 vw	2833 vw	2814 m	2676 w				$\nu_3 + \nu_{22}(B)$	
2694 vw	2694 w									$\nu_3 + \nu_{19}(B_u)$ $\nu_2 + \nu_{23}(B_u)$	$2\nu_3, 2\nu_{18}(A_g)$	Comb.	Comb.
2594 vvw													
2520 vw	2521 vw												
2426 vw	2425 m, P		2427 vw		2420 vw		2420 vw		2410 vw			$\nu_{14} + \nu_{20}(B_g)$	
2348 vw				2350 vw		2356 w						$\nu_{17} + \nu_{18}(A)/\nu_8 + \nu_7(B)$	$\nu_{10} + \nu_{17}(A)/\nu_6 + \nu_7(B)$ $\nu_8 + \nu_9(A)/\nu_5 + \nu_{17}(B)$
2320 m	2331 s, P	2334 w	2334 m	2334 m	2334 m	2333 m	2333 m			$\nu_3 + \nu_{15}(A_u)$	Comb.	Comb.	Comb.
		2314 w		2314 vw	2327 m	2314 vw	2324 m				Comb.	$2\nu_{19}(A)$	$2\nu_{18}(A)$
				2305 w									
2244 w	2243 vs, P	2246 vw	2246 s	2245 s	2240 vw	2240 vs	2240 w		2252 m	$\nu_2(a_g)$ ¹³ C	$\nu_8(a)$ ¹⁸ C	$\nu_3(a)$ ¹³ C	
1428 vs	1430 s, P	1424 s	1425 m	1428 s, sh	1420 vs	1428 s	1430 m	1420 vs	-1415 w	$\nu_4 + \nu_8(A_g)$	$\nu_{16}(b)$	$\nu_4(a), \nu_{16}(b)$	
				1420 vs	1423 m/s	1419 s	1422 s			$\nu_{19}(b_u)$	$\nu_4(a)$		
				1396 w							$\nu_3(a_g)$		
~1400 v, sh				~1380 vw, bd		1384 w				$\nu_8 + \nu_{22}(B_u)$ $\nu_{10} + \nu_{18}(B_u)$	Comb.	Comb.	
1263 vs	1267 s, P	1263 s	1266 m	1263 vs	1264 s	1266 vs	1265 m	1258 vs	1268 w	$\nu_{10} + \nu_{17}(B_u)$	$\nu_4(a_g)$	$\nu_{17}(b)$	
				1258 vs	1257 v, sh	1259 vs	1257 s	1249 s, sh		$\nu_{20}(b_u)$	$\nu_8(a)$	$\nu_8(a), \nu_{16}(b)$	
				1243 s, sh	1238 vw	1236 m, sh				$\nu_{12} + \nu_{15}(B_u)$	$\nu_{11} + \nu_{12}(A_g)$	$\nu_5(a)$	
				1205 v, w		1193 w		1220 m, sh				Comb.	
1161 vs	1172 m		~1170 w	1169 vs	1173 m	1169 vs	1170 m	1165 vs	1180?	$\nu_{14}(a_u)$	$\nu_{10}(b_g)$	$\nu_8(a), \nu_{18}(b)$	
	1162 m, D?	1163 vs		1158 vs		1158 vs	1162 m	1160 vs		$\nu_{21}(b_u)$		$\nu_{19}(b)$	
				1153 vw, sh		1153 m, sh						Comb.	
				1148 vw, sh		1148 m, sh		1137 m, sh				Comb.	
		1093 m				1092 m						Comb.	
						972 w						$\nu_8 + \nu_{11}(A)$	
						969 w						$\nu_{21} + \nu_{23}(A)$	
905 m	903 m, D?	903 m	902 w	907 m	899 vw	905 m	905 m	907 s	906 w	$\nu_{18}(a_u)$	$\nu_{11}(b_g)$	$\nu_7(a), \nu_{20}(b)$	
		864 vw, bd		904 w, sh		860 vw						$\nu_{21} + \nu_{24}(A)$	
				844 v, w				841 vw				$\nu_{20} + \nu_{23}(A)$	
782 m	785 s, P		784 m			782 s							
		776 m		769 w	773 w, sh	770 s	773 s	795 vw, bd				$\nu_8(a)$	
	759 w, sh	760 m		750 w		751 s	754 m					$\nu_{22} + \nu_{23}(A)$	
							708 s					$\nu_{10} + \nu_{11}(A)$	
702 vs	699 vs, P	705 vs	697 vs	701 vs	698 vs	705 vs	697 vs	715 vs	707 s	$\nu_{22}(a_u)$	$\nu_8(a_g)$	$\nu_{21}(b)$	
		690 vs		690 w, sh	685 w, sh	692 vs	690 vs	693 s, sh				$\nu_8(a)$	
				680 w, sh		677 w, sh	679 w					$\nu_{10} + \nu_{23}(B)$	
~545 vw	~560 vvw	566 w, bd		~550 w, bd		562 m		558 m		$\nu_{12} + \nu_{16}(B_u)$		$\nu_{11} + \nu_{23}(B)$	
~490 m		498 vw		484 w		484 s	484 m/w					$\nu_{22}(b)$	
	~450 m, P	~455 w	~450 m/w		455 m					$\nu_7(a_g)$			
												$\nu_{21}(b)$ $\nu_{10}(a)$	

Table 1. Continued

Liquid		Amorphous (90 K)		Crystal I (90 K)		Crystal II (90 K)		Crystal I high pressure		Assignments ^a			
IR	Raman	IR	Raman	IR	Raman	IR	Raman	IR	Raman	C_{2h}	C_2	D_{2h}^*	
~430 m	~425 m, sh	429 w 410 vw	~430 m/w	425 s		411 vw	412 s	440 vs		$\nu_{23}(b_u)$			} $\nu_{11}(a), \nu_{22}(b)$
~280 sh	~330 m, D ~300 m, sh	~290 w 272 vw	~340 m/w ~290 m/w	292 w ~275 w	341 m	290 vs	288 s 273 vs 266 w, sh		344 m	$\nu_{12}(b_g)$	$\nu_{10}(a)$ $\nu_{11}(a)$ $\nu_{25}(b)$ $\nu_8 + \nu_{12}(A)$		
~210 m		~235 m 198 vw		210 s				~235 w		$\nu_{16}(a_u)$			
~120 m	~125 m/s	~150 m 106 vw	~145 m	160 w 126 m	165 s/vs	158 s	150 s	150 w 120 s		$\nu_{24}(b_u)$	$\nu_8(a_g)$ $\nu_{24}(b)$		} $\nu_{12}(a), \nu_{23}(b)$
		86 vw		97 s		113 m 109 m	113 s 109 s			$\nu_{17}(a_u)$	Lattice	$\nu_{12}(a)$	
						88 s	89 s				Lattice	Lattice	
						75 s	75 s				Lattice	Lattice	
						72 s					Lattice	Lattice	
		~60 vw		58 vw 53 vw		62 s	67 s 60 s 54 s			Lattice Lattice		Lattice Lattice Lattice	
~40 w		~30 vw		40 vw	49 m					Lattice			Lib.

^a Assignments made to C_{2h} (crystal I), C_2 (crystal II) and D_{2h}^* (liquid).

^b Abbreviations: s, strong; m, medium; v, very; bd, broad; sh, shoulder; P, polarized; D, depolarized.

Table 2. Fundamentals for DCB in crystal I (*anti* conformer)

Description ^a	Species No.	Wavenumbers (cm ⁻¹)	
		Observed ^b	Calculated ^c
CH ₂ sym.str.	<i>a_g</i> ν_1	2956	2963
C≡C str.	ν_2	2245	2241
CH ₂ scissor	ν_3	1417	1454
CH ₂ wag	ν_4	1264	1250
C-C sym.str.	ν_5	782	788
C-Cl sym.str.	ν_6	698	699
Skel.bend	ν_7	455	462
Skel.bend	ν_8	165	140
CH ₂ asym.str.	<i>b_g</i> ν_9	3002	2994
CH ₂ twist	ν_{10}	1173	1158
CH ₂ rock	ν_{11}	899	914
CCCC bend	ν_{12}	341	343
CH ₂ asym.str.	<i>a_u</i> ν_{13}	2998	2995
CH ₂ twist	ν_{14}	1169	1166
CH ₂ rock	ν_{15}	907	914
CCCC bend	ν_{16}	210	197
Torsion	ν_{17}	97	—
CH ₂ sym.str.	<i>b_u</i> ν_{18}	2958	2963
CH ₂ scissor	ν_{19}	1420	1455
CH ₂ wag	ν_{20}	1258	1255
C-C asym.str.	ν_{21}	1158	1168
C-Cl asym.str.	ν_{22}	701	704
Skel.bend	ν_{23}	425	394
Skel.bend	ν_{24}	126	84

^a From the largest term in the potential energy distribution (PED).

^b Wavenumbers observed in the crystal.

^c Force field from Ref. 12.

Table 3. Fundamentals for DCB in crystal II (*gauche* conformer)

Description ^a	Species No.	Wavenumbers (cm ⁻¹)	
		Observed ^b	Calculated ^c
CH ₂ asym.str.	<i>a</i> ν_1	2992	2995
CH ₂ sym.str.	ν_2	2952	2963
C≡C str.	ν_3	2240	2241
CH ₂ scissor	ν_4	1419	1454
CH ₂ wag	ν_5	1259	1250
CH ₂ twist	ν_6	1169	1168
CH ₂ rock	ν_7	905	904
C-C sym.str.	ν_8	770	791
C-Cl sym.str.	ν_9	692	699
Skel.def.	ν_{10}	412 ^d	433
Skel.def.	ν_{11}	288 ^d	277
Skel.def.	ν_{12}	109 ^d	79
Torsion	ν_{13}	75 ^d	—
CH ₂ asym.str.	<i>b</i> ν_{14}	2992	2995
CH ₂ sym.str.	ν_{15}	2952	2963
CH ₂ scissor	ν_{16}	1428	1459
CH ₂ wag	ν_{17}	1266	1252
CH ₂ twist	ν_{18}	1169	1170
C-C asym.str.	ν_{19}	1158	1159
CH ₂ rock	ν_{20}	905	915
C-Cl asym.str.	ν_{21}	705	706
Skel.def.	ν_{22}	484	509
Skel.def.	ν_{23}	267 ^d	263
Skel.def.	ν_{24}	150 ^d	134

^a From the largest term in PED.

^b Wavenumbers observed in IR spectra of the crystal except where noted.

^c Force field from Ref. 12.

^d Values from Raman spectra of the crystal.

syn was observed for 1,4-difluorobut-2-yne in the vapour).

Some partial interpretations of the DCB liquid-phase spectra supported by force constant calculations¹⁵ have been reported^{10,11} in the region above 300 cm⁻¹. Earlier assignments of the crystal spectra of the *anti*^{15,16} and *gauche*¹⁶ conformers were also supported by normal coordinate analyses. However, lacking the far-IR spectra of the two crystals,^{15,16} the low-frequency bending and torsional modes of the *anti* were unassigned. The *gauche* fundamentals based on Raman spectra alone¹⁶ are also in need of revision. Our assignments above 500 cm⁻¹ are in reasonably good agreement with those of the earlier workers^{15,16} and need not be discussed.

The broad IR and Raman bands of the liquid and of the amorphous solid at temperatures as low as 90 K are interpreted as coinciding *a* and *b* fundamentals of the *D*_{2h}^{*} Ms group.²⁶ The appearance or disappearance of IR and Raman bands in crystals I and II makes the assignments to *anti* and *gauche* straightforward in most cases. Hence, Raman bands with no IR counterparts at 455, 341 and 165 cm⁻¹ and IR bands with no Raman analogues at 425, 210, 126 and 97 cm⁻¹ of the crystal I spectrum are definitely *anti* fundamentals (Table 2). Coinciding IR and Raman bands at 484, 411, 290, 273, 158, 113 and 75 cm⁻¹ of the crystal II spectra are assigned as *gauche* fundamentals.

A number of IR and Raman bands below 100 cm⁻¹ present in the crystal spectra but absent from those of

the liquid are interpreted as lattice modes. As is apparent from Table 1 all the assigned lattice modes of crystal I are present either in IR or in Raman but not in both spectra, suggesting a symmetry centre in the unit cell. The low-frequency spectra of crystal II are less conclusive, since some IR bands have Raman counterparts and some do not. The strong IR band at 97 cm⁻¹ in crystal I and the intense IR and Raman bands at 75 cm⁻¹ in crystal II were tentatively interpreted as the torsional modes of the *anti* and *gauche* conformers, respectively. Our value for the *gauche* conformer is in reasonable agreement with *ca* 67 cm⁻¹ for the torsion reported by Suzuki¹⁶ from neutron scattering data. However, a clear distinction between the torsional mode and the lattice modes cannot be made from our spectra, particularly since no torsional modes are expected in the liquid or amorphous phases. The broad weak IR band at 40 cm⁻¹ in the liquid (30 cm⁻¹ in the amorphous phase) was interpreted as a librational mode. The assigned fundamentals for the *anti* and *gauche* conformers agree fairly well with the calculated values. Moreover, the fundamentals are in good agreement with those of 1,4-difluorobut-2-yne³ and 1,4-dibromobut-2-yne.² In all three dihalobutyne the CH₂X stretching and bending modes have negligible mechanical coupling across the C—C≡C—C frame. Hence, the in-phase motions of species *a_g* and *a_u* (*anti*) and *a* (*gauche*) coincide with the out-of-phase motions *b_g* and *b_u* and *b* through the spectrum.

Normal coordinate calculations

The normal modes of vibrations for the *anti* and *gauche* conformations of DCB given in Tables 2 and 3, respectively, were calculated using the structural parameters and force constants listed in Ref. 12. Obviously, only minor adjustments in the force constants would be necessary in order to obtain a perfect agreement with

the observations. However, this is outside the scope of this work.

Acknowledgements

The authors are grateful to P. Fostervoll and G. Isaksen for recording the x-ray and DSC data, respectively, and to A. Horn for drawing the figures.

REFERENCES

1. K. Kveseth, Doctoral Thesis, University of Oslo (1970).
2. O. H. Ellestad and K. Kveseth, *J. Mol. Struct.* **25**, 175 (1975).
3. A. Karlsson, P. Klæboe, K.-M. Marstokk, H. Møllendal and C. J. Nielsen, *Acta Chem. Scand., Ser. A* **40**, 374 (1986).
4. Y. Morino, I. Miyagawa and A. Wada, *J. Chem. Phys.* **20**, 1976 (1952).
5. Y. Morino, I. Miyagawa, T. Chiba and T. Shimozawa, *Bull. Chem. Soc. Jpn.* **30**, 222 (1957).
6. K. Kuchitsu, *Bull. Chem. Soc. Jpn.* **30**, 391, 399 (1957).
7. B. L. Barton, *J. Chem. Phys.* **51**, 4670 (1969).
8. A. Valette, *Ann. Chim. (Paris)* **3**, 677 (1948).
9. J. L. H. Allan, G. D. Meakins and M. C. Whiting, *J. Chem. Soc.* 1874 (1955).
10. B. Bak, J. J. Christiansen and E. Madsen, *Acta Chem. Scand.* **14**, 573 (1960).
11. G. A. Crowder, *J. Mol. Struct.* **12**, 302 (1972).
12. F. Lichene, G. Dellepiane and V. Lorenzelli, *J. Chem. Phys.* **70**, 4786 (1979).
13. F. Lichene, G. Dellepiane and M. Gussoni, *J. Chem. Phys.* **40**, 163 (1979).
14. L. Mannik, P. A. Sipos and M. K. Phibbs, *Can. J. Spectrosc.* **21**, 105 (1976).
15. P. A. Sipos and M. K. Phibbs, *Can. J. Spectrosc.* **21**, 69 (1976).
16. S. Suzuki, *J. Mol. Struct.* **46**, 155 (1978).
17. F. A. Miller and B. M. Harney, *Appl. Spectrosc.* **24**, 291 (1970).
18. B. O. Myrvold and P. Klæboe, *Acta Chem. Scand., Ser. A* **39**, 733 (1985).
19. C. N. R. Rao and K. J. Rao, *Phase Transitions in Solids*. McGraw-Hill, New York (1978).
20. S. D. Christian, J. Grundnes and P. Klæboe, *J. Chem. Phys.* **65**, 496 (1976).
21. S. D. Christian, J. Grundnes, P. Klæboe, C. J. Nielsen and T. Woldbaek, *J. Mol. Struct.* **34**, 33 (1976).
22. T. Woldbaek and P. Klæboe, *J. Mol. Struct.* **63**, 195 (1980), and references cited therein.
23. T. Woldbaek, C. J. Nielsen and P. Klæboe, *J. Mol. Struct.* **66**, 31 (1980).
24. S. D. Christian, J. Grundnes and P. Klæboe, *J. Am. Chem. Soc.* **97**, 3865 (1975).
25. P. Klæboe, M. Moneeb, E. Tørneng, H. Hopf, I. Bøhn, B. N. Cyvin and S. J. Cyvin, *Z. Naturforsch., Teil A* **35**, 537 (1980).
26. P. R. Bunker, *Molecular Symmetry and Spectroscopy*. Academic Press, London (1979).
27. F. D. Saeva (Ed.), *Liquid Crystals*. Marcel Dekker, New York (1979).
28. J. W. Emsley, G. R. Luckhurst and C. P. Stockley, *Proc. R. Soc. London, Ser. A* **381**, 117 (1982).
29. B. O. Myrvold and P. Klæboe, *Spectrochim. Acta, Part A* **42**, 1035 (1986).
30. G. Dellepiane and M. Gussoni, *J. Mol. Spectrosc.* **47**, 515 (1973).